JOURNAL OF MATERIALS SCIENCE 30 (1995) 1144–1150

Three-dimensional cellular automaton models of microstructural evolution during solidification

S. G. R. BROWN, N. B. BRUCE
Materials Engineering, University College Swansea, Singleton Park, Swansea SA2 8PP, UK

The evolution of microstructural features during solidification involves complex interactions between several physical phenomena. Cellular automata (CA) models are often characterized as being simple in their construction and yet able to produce very complicated behaviour. This property of CA models has been exploited to produce computer simulations of various aspects of microstructural evolution occurring during solidification. Results of a series of three-dimensional simulations of non-isothermal "free" dendritic growth are presented and the changes in dendrite morphology for different conditions are quantified and discussed. A modification of this model was also developed to examine the effects of composition on microstructural evolution for a simple eutectic system. As the composition moves towards the eutectic the simulated microstructures change from combined dendritic/lamellar to completely lamellar.

1. Introduction

For cast metallic materials the nature of the microstructure that evolves during solidification can significantly affect the properties of the as-solidified material. Dendrite morphology, fragmentation and interdendritic fluid flow can affect the final as-cast grain size, the distribution of porosity, solute segregation and as-cast mechanical properties. In metallic alloys the coupled growth of two or more phases may also occur. A typical example being eutectic growth where, during solidification, the liquid phase transforms to two solid phases that grow in a coupled manner.

Understanding the wide variety of growth morphologies observed in solidifying systems has been an active and engrossing field of study for many decades. At present, several analytical and numerical models exist that attempt to describe various aspects of these phase transformations. In this paper the cellular automaton (CA) approach is used to model both dendritic and coupled growth behaviour. Construction of CA models is relatively straightforward and at first sight the principles underlying the models appear simplistic. However, CA models are very useful in situations where there are complicated interactions occurring between different physical phenomena. In these situations they are capable of producing results of surprising complexity.

1.1. Dendritic growth

Materials with low entropies of fusion often display dendritic growth behaviour during solidification. A dendrite is a branching structure with projections or side arms that grow in particular crystallographic directions. The growth of dendrites during solidification is the result of interactions between various physical phenomena. These include the effects of heat transfer, evolution and removal of latent heat, the effect of curvature of the solid/liquid interface on the local freezing temperature, mechanisms of atom attachment to the growing solid interface and the solid/liquid interfacial energy. In alloys, the rejection of solute during freezing also influences the local liquidus temperature.

Earlier theories of dendritic growth are concerned with the growth of isolated, branchless dendrites growing in supercooled one-component systems [1–11]. This type of growth is termed "free" dendritic growth where the latent heat of fusion evolved during freezing flows into the supercooled liquid. In these models the dendrite is usually assumed to be a simple shape (e.g. a parabola of revolution) that grows in a shape-preserving manner. These models have been used to investigate the relationships between supercooling and growth rate. More recent theories [12–17] have attempted to describe the growth of branchless cellular and dendritic arrays in positive-temperature gradients, i.e. "constrained" growth. In these models the relationships between alloy composition, radius of curvature at the dendrite tip, temperature gradient, growth rate and primary dendrite arm spacings have been investigated.

Numerical models of dendritic growth were initially applied to the growth of "free" dendrites in supercooled one-component systems [18–23]. More recently, attempts have been made to model the evolution of alloy dendrites using a technique termed the phase-field method [24].

0022–2461

The growth of "free" dendrites is influenced by two main factors. The first is the effect of the radius of curvature of the solid/liquid interface on the local equilibrium freezing temperature. This is known as the Gibbs–Thomson effect. The local solid/liquid interface curvature (assuming the solid/liquid interface is convex towards the liquid) depresses the local equilibrium freezing temperature according to the expression

$$\Delta T = \frac{\sigma T_m}{\Delta H \rho}\left(\frac{1}{R_1} + \frac{1}{R_2}\right) \quad (1)$$

where T_m is the equilibrium freezing temperature of a planar interface, σ is the solid–liquid interfacial energy, R_1 and R_2 are the radii of curvature of the surface in two directions at right angles, ΔH is the enthalpy of fusion and ρ is the density of the solid.

The second factor to influence freezing is the release of latent heat during solidification. This heat must be removed from the interface to allow further growth to occur.

Several two-dimensional numerical models already exist that incorporate these two factors into computer simulations. In terms of simulating the evolution of dendrite morphology, one numerical model of "free" dendritic growth showed small periodic perturbations in the solid/liquid interface of a growing dendrite tip that were attributed to slight oscillations in tip velocity [20]. In contrast, two-dimensional phase-field models have produced pronounced side-arm growth in reported simulations although this behaviour was influenced by the magnitude of deliberately induced random noise in the temperature field [21, 22]. This result suggests that side branching may be controlled by mechanisms not directly connected to the conditions at the advancing dendrite tip.

1.2. Coupled growth

There is a variety of phase transformations involving coupled growth processes that may or may not involve the presence of a liquid phase. This paper will confine itself to two-component systems with a eutectic reaction occurring during solidification that can be described by the general expression

$$\text{Phase X} \rightarrow \text{Phase Y} + \text{Phase Z} \quad (2)$$

This type of transformation proceeds by a two-stage process of nucleation and growth. Nucleation usually occurs near the container walls and growth proceeds in the opposite direction to the direction of heat removal. During growth, the Y and Z phases grow in a coupled manner. As the transformation occurs, the atomic/molecular species rejected at the growing interfaces must be redistributed by diffusion to facilitate the coupled growth.

Most theoretical studies of coupled growth have been concerned with steady-state transformations of, for example. eutectoids or eutectics [25–27]. Experimental investigations of unidirectional coupled growth of eutectics under steady-state conditions have also been undertaken [28–30]. As is the case with dendritic growth, attempts have been made to develop numerical models of coupled growth behaviour. A boundary element approach has been used to investigate the relationships between growth conditions and lamellar spacings [31] and random walk models have been used to investigate non-steady-state growth morphologies in eutectics [32] and general binary systems [33].

2. The cellular automaton models

The two CA models described below operate on a regular lattice of cubic elements. Each element is defined by an integer value as being either solid or liquid. Each element can be further defined by having a particular temperature or alternatively a particular composition associated with it. Initially, all sites on the lattice are defined as liquid sites except those sites that are preset as solid sites at the beginning of the simulation to represent nuclei.

2.1. A three-dimensional non-isothermal "free" dendritic growth model

In previous work, a two-dimensional CA model of non-isothermal "free" dendritic growth has been used to model columnar and equiaxed dendritic growth morphologies [34], to investigate the relationship between initial liquid supercooling and growth rate [35] and examine the variation in two-dimensional growth morphology for different initial liquid supercoolings [36]. In this paper, a three-dimensional version of this model is used to simulate "free" dendritic growth for different initial liquid supercoolings and to quantify the different growth morphologies obtained for the different conditions.

The basis of the CA model is a simple approximation to the Gibbs-Thomson effect. In the current "free" dendrite simulations a one million element grid was used (i.e. $100 \times 100 \times 100$ elements) with an initial nucleus of $3 \times 3 \times 3$ elements placed at the centre. Each of these was set to a value of 1 (i.e. solid). All other elements were initially set to 0 (i.e. liquid). For each simulation the temperatures of all sites were also set to an initial predetermined value representing supercooling. Opposite faces of the cubic $100 \times 100 \times 100$ computational domain were treated as periodic, i.e. as if in contact with one another. Details of the simulation procedure are summarized below assuming that the dendrites are thermal in nature.

The following rules and conditions were assumed:

(a) a liquid site may transform to a solid site only if $s_x \geqslant 3$ and/or $s_y \geqslant 3$, and/or $s_z \geqslant 3$, (where s_x, s_y and s_z are the number of solid sites present in the surrounding eight nearest neighbours taken in each of the principal x, y and z planes, respectively);

(b) growth at a particular site will only occur if the temperature of the liquid site is less than a critical temperature, T_{crit};

(c)

$$T_{crit} = -\gamma[f(s_x) + f(s_y) + f(s_z)] \quad (3a)$$

where

$$f(s_i) = \frac{1}{s_i} \qquad s_i \geqslant 1 \tag{3b}$$

$$f(s_i) = 0 \qquad s_i < 1 \tag{3c}$$

where γ is a constant representing the solid/liquid interfacial energy;

(d) when a liquid element transforms to a solid element the temperature of the element is raised to a fixed value to simulate the release of latent heat [34];

(e) conductive heat transfer is modelled by updating the temperature of each element at each time step. The mean temperature of the six nearest neighbour elements is computed and the temperature of the central element is moved towards this average by an amount governed by an assumed heat transfer constant [34]. Convective heat flow was not modelled.

For all "free" dendrite simulations, γ was set to a value of 20. Equation 3a provides for the effects of interface curvature in a simple manner. In each step of the simulation all liquid sites are tested to determine whether growth will occur. All sites are then updated simultaneously to their new states of liquid or solid. Liquid sites that have transformed to solid have their temperatures raised to a fixed value and finally two heat-transfer steps are performed. The process is then repeated.

Simulations were carried out for a series of initial liquid supercoolings ranging from -60 to -32. In each case the dendrite was allowed to grow until it reached a certain fixed length along any of the principal axes. The fineness of the dendritic structure produced was quantified by calculating the volume to surface area ratio of the solid for each of the simulated dendrites.

2.2. A three-dimensional cellular automaton model of coupled growth

The coupled-growth CA model is based on similar principles to the dendritic growth model except that individual elements are now defined as being either liquid, solid of phase Y or solid of phase Z [37]. Each liquid element is further defined with its own particular composition. Heat transfer is not simulated. The model assumes a hypothetical two-component system described by a symmetrical phase diagram as shown in Fig. 1. In the model the eutectic composition is defined as zero, Y phase cells have a value of -100 and Z phase cells have a value of 100. All other cells with values in the range > -100 to < 100 are liquid cells. Again, all initially solid sites representing nuclei are preset at the beginning of the simulation. The simulation then proceeds as a series of growth, solute rejection and diffusion steps.

The grid used for these simulations was a $150 \times 150 \times 10$ lattice of cubic elements. The 150×10 base of the grid was initially completely covered in Y and Z phase elements placed randomly. All liquid elements were then set to the value of the bulk liquid composition. In this paper, two bulk liquid compositions were used, 0 and 20.

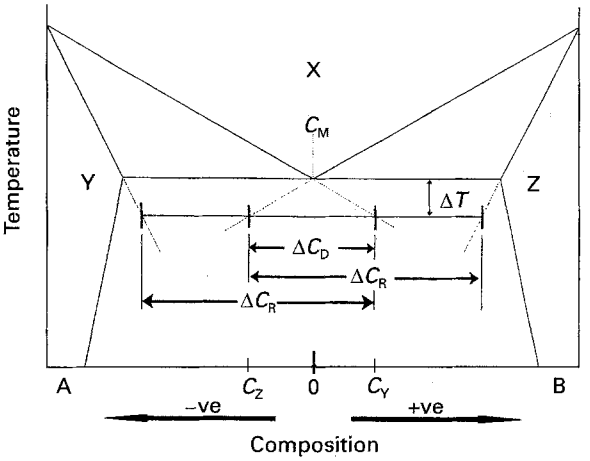

Figure 1 Hypothetical phase diagram used as the basis of the cellular automaton model of coupled growth.

An important feature of coupled-growth processes is the variation in composition that exists in the liquid near the growing interface. This compositional variation changes progressively from a maximum of C_y and C_z at the centres of the freezing Y and Z particles, respectively, to the bulk liquid composition at the Y–Z phase boundaries. $\Delta C_O = C_y - C_z$ provides the driving force for interdiffusion.

The composition profiles that develop during the simulation do so naturally and morphological features of the developing structures in the simulation, such as interparticle spacing, cannot be predetermined. The establishment and maintenance of a compositional profile across the interface must be controlled by the model. Using a similar approach to the dendritic model above, growth is determined by using critical values of composition related to the number of nearest neighbours of a particular phase. Thus, a liquid element will transform to a Y phase element once its composition drops to a critical value, $C_{crit\,y}$, or lower. Similarly, if the composition of a liquid site rises to $C_{crit\,z}$ or higher it can transform to a Z phase element. $C_{crit\,y}$ and $C_{crit\,z}$ are both functions of the number of nearest neighbour Y and Z phase elements, respectively

$$C_{crit\,y} = fn(N_y) \tag{4}$$

$$C_{crit\,z} = fn(-N_z)$$

where N_y and N_z are the number of nearest neighbour Y and Z phase elements, respectively. The simulation proceeds according to the following steps.

(a) Growth: each liquid element is tested to determine whether it will transform to either the Y or Z phase. The composition C_E of the element and both N_Y and N_Z are determined.

If $N_Y > N_Z$ and $N_Y \geqslant 6$ and $C_E \leqslant C_{crit\,y}$, then the element will transform to a Y phase element.

If $N_Z > N_Y$ and $N_Z \geqslant 6$ and $C_E \geqslant C_{crit\,z}$, then the element will transform to a Z phase element.

The value of 6 ensures sensible structures are produced.

(b) Solute rejection: all liquid elements that will transform to Y phase elements have their compositions changed to a fixed positive value, R. All liquid elements that will transform to Z phase elements have their compositions set to a fixed negative value, $-R$. This adjustment in composition is used to represent the rejection of atomic/molecular species by the growing phase caused by the difference in composition, ΔC_R in Fig. 1, between the product phase and the liquid composition, from which it is forming. Because of the symmetry of the phase diagram the same value, R, is used for both Y and Z phases. (It should be noted that this is a simplification. In reality, the compositional variation across the interface will cause different ΔC_R values at different positions on the growth surface. In a real physical system, to maintain isothermal growth a variation in interface curvature would be required to offset the compositional variation ahead of the interface.)

At this stage the elements do not transform, they are only allocated Y or Z phase identities after the diffusion routine below is completed.

(c) Diffusion: at this point the liquid elements that will transform to solid have been adjusted to model the redistribution of atomic/molecular species. The diffusion of these species in the liquid is now simulated. Each liquid element is sampled in turn. For any given liquid element, the local average composition of its nearest neighbour liquid elements is calculated. The composition of all liquid elements is then adjusted simultaneously towards their local average value by an amount controlled by an assumed diffusion coefficient. When this procedure is complete, all those elements that had previously been considered able to transform are given the identification of either Y or Z phase elements. The next growth step is then begun. This model was used to simulate coupled growth behaviour for two different initial bulk liquid compositions. Because no nucleation occurs after the simulation is begun, a three-dimensional grid has been used to reduce the likelihood of one phase completely overgrowing the other and to allow adjustments in particle spacings to occur as growth proceeds.

3. Results

Simulated dendritic structures are shown in Figs 2 and 3; in all cases, certain portions of the dendrite have been cut away to reveal the internal structure. In Fig. 2a–f the development of a three-dimensional dendritic structure is shown at different stages during growth. In this case, the initial supercooling in the liquid was set at -58 and a dense growth morphology with a high volume fraction of solid is observed. Fig. 3a–f show simulated dendritic structures for initial liquid supercoolings of -55, -50, -45, -40, -37 and -32,

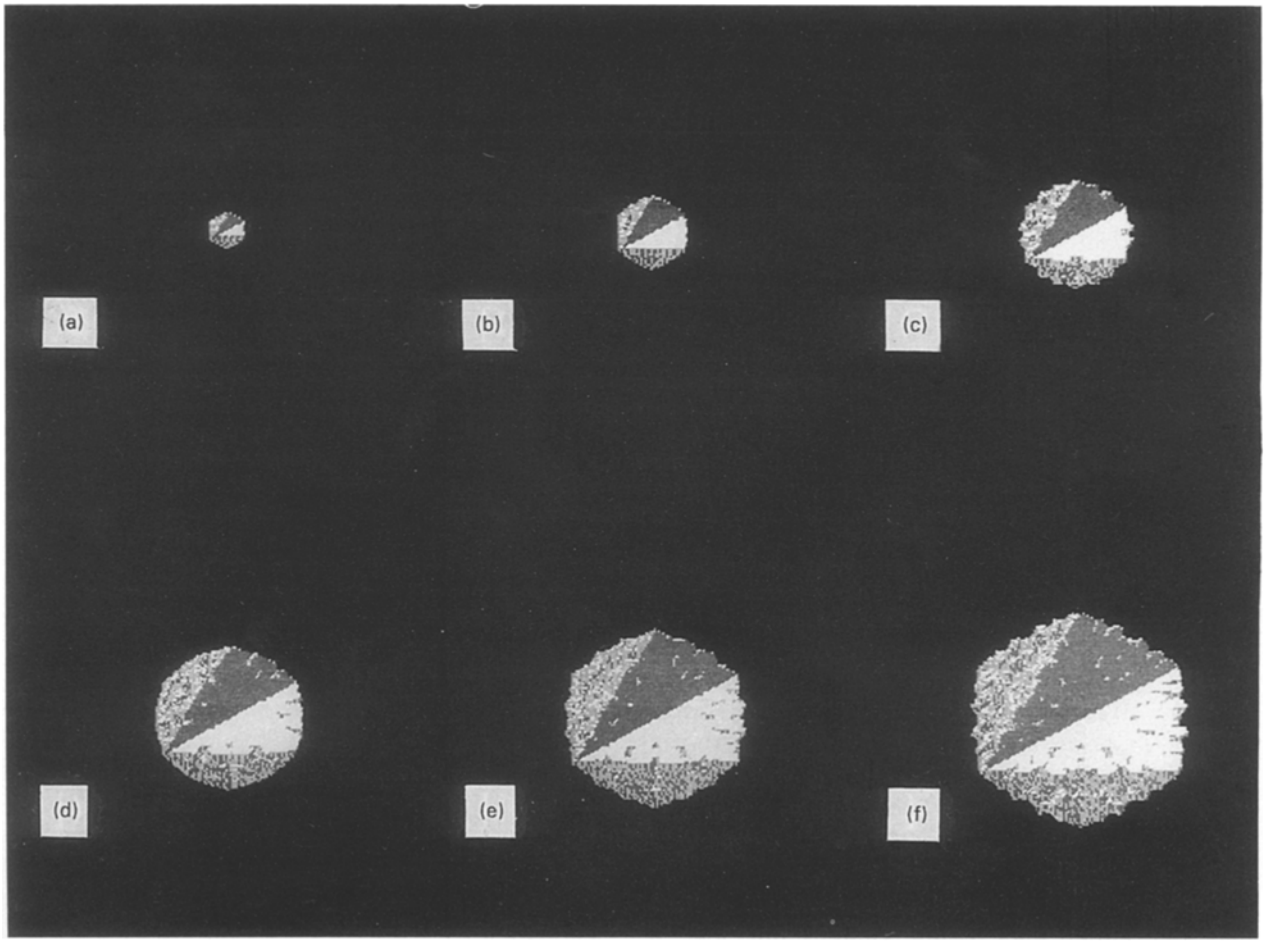

Figure 2 The evolution (from a–f) of a three-dimensional dendritic structure, the top right-hand quadrant has been removed to reveal the internal structure.

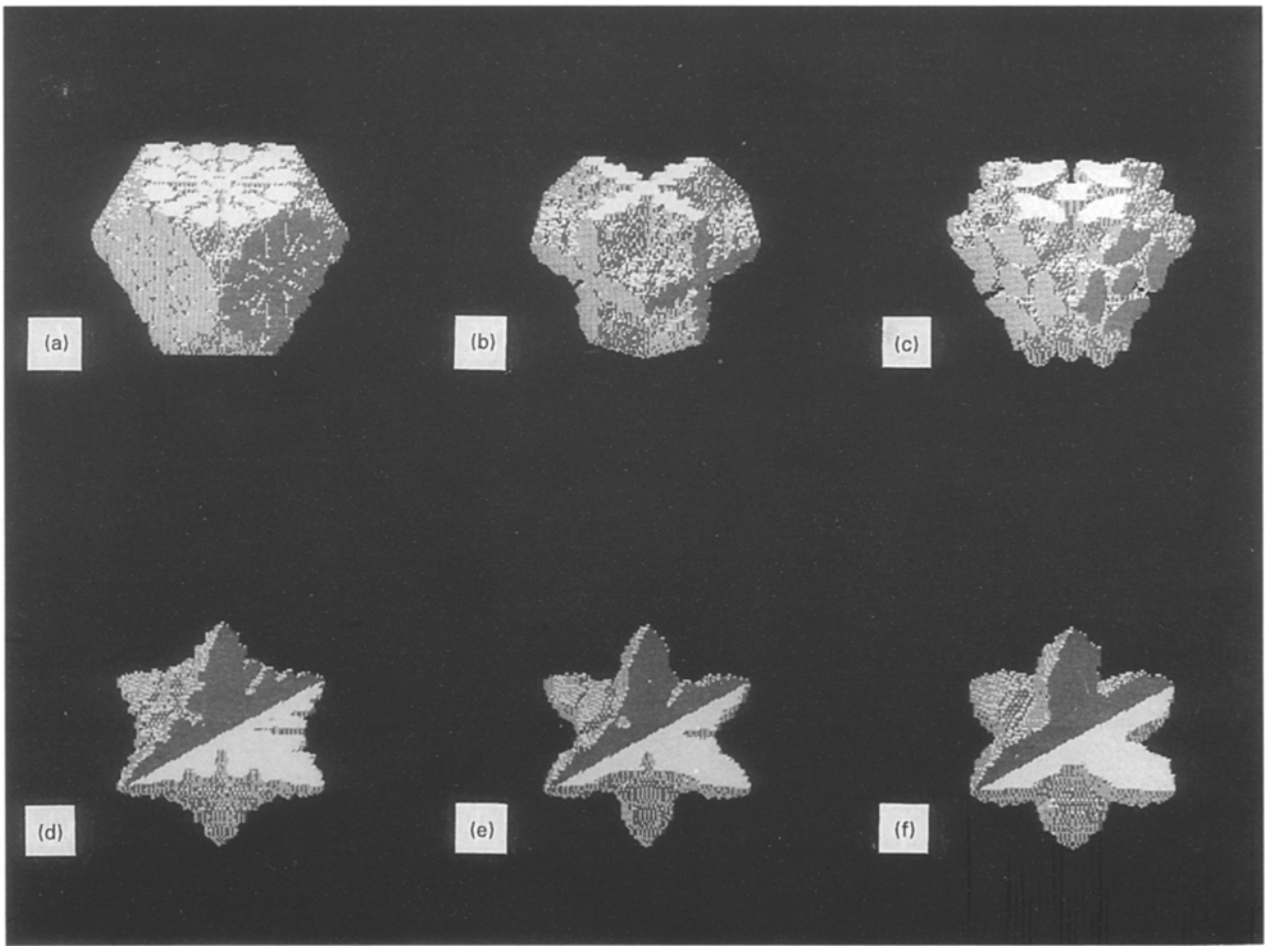

Figure 3 Dendritic structures produced for initial liquid supercoolings of (a) − 55, (b) − 50, (c) − 45, (d) − 40, (e) − 37 and (f) − 32. Certain portions of the dendritic structures have been removed to reveal the internal structures.

respectively. Fig. 3a again shows a dense growth morphology, whereas in Fig. 3b a plate-like growth morphology is observed. Tip instability is observed in Fig. 3c where many dendrite arms have developed and grown radially from the central nucleus. Fig. 3d–f show a progression to coarser dendritic growth behaviour with decreasing amounts of side branching.

Fig. 4 shows the calculated volume-to-surface area ratios for a series of dendrite simulations carried out for liquid supercoolings in the range − 60 to − 32. The volume-to-surface area ratio has been used to quantify the "fineness" of the dendritic structures produced. With decreasing amounts of supercooling a coarse–fine–coarse trend is observed.

Results of coupled growth simulations are shown in Fig. 5a–f. In this figure growth has begun at the 150 × 10 base of the grid and continued upwards. Fig. 5a–e shows the development of a combined dendritic/lamellar structure at various stages of development for an initial bulk liquid composition of 20, i.e. off-eutectic. Dendritic projections into the liquid can be seen clearly. Fig. 5f shows the structure produced for the same conditions except that the initial bulk liquid composition was 0, i.e. eutectic. Here the growth morphology is only lamellar.

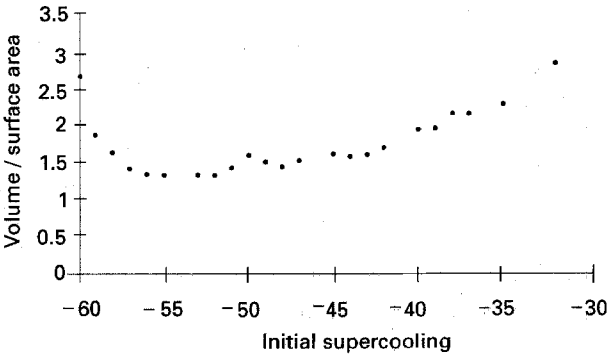

Figure 4 The calculated volume-to-surface area ratio for simulated dendritic structures with initial liquid supercoolings ranging from − 60 to − 32.

4. Discussion

It has been observed experimentally for thermal dendrites that increased supercooling leads to finer dendritic growth behaviour [38]. The results in Fig. 3c–f agree with this observation.The coarser structures observed at larger initial liquid supercoolings (e.g. Figs 2a–f and 3a) may be attributable to the finite size of the discrete underlying grid of elements used in the simulations.

The coupled growth results in Fig. 5a–f are particularly pleasing in two respects. First, a lamellar

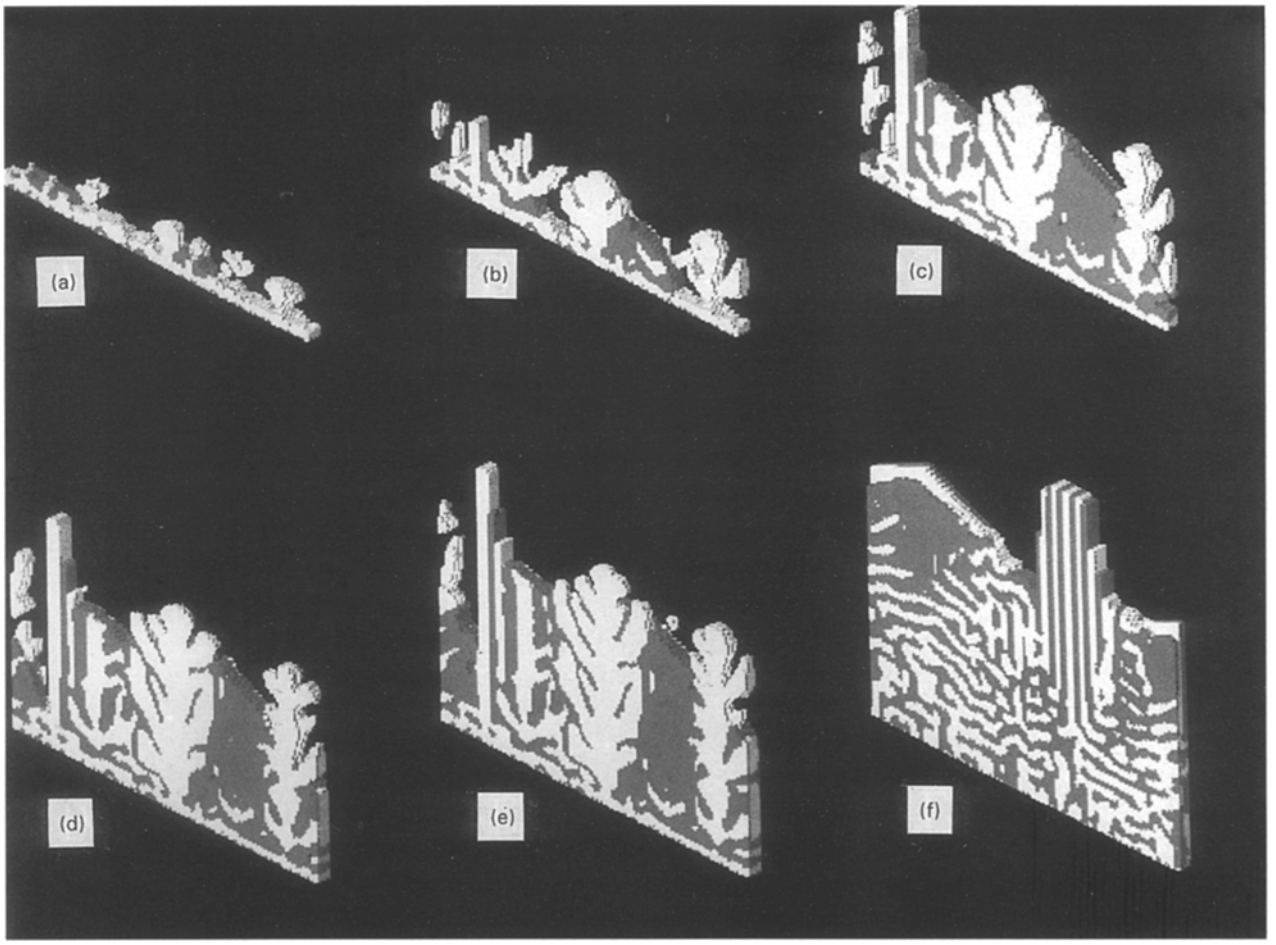

Figure 5 The development of a combined dendritic/lamellar structure (a–e) compared to a fully lamellar structure (f). The structure developing in (a–e) was for an off-eutectic composition, the structure in (f) was for the eutectic composition.

structure, commonly observed in practice, has evolved naturally. Secondly, when simulating freezing in a liquid of off-eutectic composition, the proportion of the Y and Z phases present is not the same and definite dendritic behaviour is observed in the major phase. In reality, the length scales associated with the coupled growth behaviour would often be much smaller than those associated with dendritic growth. This again may be attributable to the discrete nature of the underlying grid.

Despite the simplicity of their construction, the three-dimensional CA models used in this work have been able to display complicated growth behaviour similar to that often observed in real systems. Although it should be noted that the models are only presented as examples. The simplicity of the CA approach means that complex three-dimensional structures can be generated in a matter of a few hours using low-cost PC hardware. This advantage is perhaps offset by the qualitative, or at best semi-quantitative [35], nature of the method as it has been developed to date. Certainly CA models represent a potentially powerful tool to improve the ability to model and understand the evolution of microstructure during solidification. Yet, to achieve their full potential, CA models must now be developed further to become significantly more quantitative in nature.

5. Acknowledgement

This work was carried out as part of the EPSRC-funded research project reference number GR/J28575.

References

1. B. CHALMERS, "Principles of Solidification" (Wiley, New York, 1964) Ch. 4.
2. G. P. IVANTSOV, *Dokl. Acad. Nauk.* **58** (1947) 567.
3. D. E. TEMKIN, *ibid.* **132** (1960) 1307.
4. G. HORVAY and J. W. CAHN, *Acta Metall.* **9** (1961) 695.
5. G. F. BOLLING and W. A. TILLER, *J. Appl. Phys.* **32** (1961) 2587.
6. M. E. GLICKSMAN and R. J. SCHAEFFER, *J. Crystal Growth* **1** (1967) 297.
7. L. A. TARSHIS and G. R. KOTLER, *ibid.* **2** (1968) 222.
8. R. F. SEKERKA, R. G. SEIDENSTICKER, D. R. HAMILTON and J. D. HARRISON, in "Investigation of Desalination by Freezing" (Westinghouse Research Laboratory Report, 1967).
9. E. G. HOLTZMANN, *J. Appl. Phys.* **41** (1970) 1460.
10. R. TRIVEDI, *Acta Metall.* **18** (1970) 287.
11. G. E. NASH and M. E. GLICKSMAN, *ibid.* **22** (1974) 1283.
12. M. H. BURDEN and J. D. HUNT, *J. Crystal Growth* **22** (1974) 109.
13. I. JIN and G. R. PURDY, *ibid.* **23** (1974) 29.
14. J. S. KIRCALDY, *Scripta Metall.* **14** (1980) 739.
15. R. TRIVEDI, *J. Crystal Growth* **49** (1980) 219.
16. W. KURZ and J. D. FISHER, *Acta Metall.* **29** (1981) 11.
17. V. LAXMANAN, *ibid.* **33** (1985) 1023.

18. W. OLDFIELD, in "The Solidification of Metals" (The Iron and Steel Institute, London, 1968) p. 70.
19. W. OLDFIELD, *Mater. Sci. Eng.* **11** (1973) 211.
20. J. D. HUNT, *Acta Metall. Mater.* **39** (1991) 2117.
21. R. KOBAYASHI, *Phys. D* **63** (1993) 410.
22. A. A. WHEELER, B. T. MURRAY and R. J. SCHAEFFER, *ibid.* **66** (1993) 243.
23. S. L. WANG, R. G. SEKERKA, A. A. WHEELER, B. T. MURRAY, S. R. CORIELL, R. J. BRAUN and G. B. McFADDEN, *ibid.* **69** (1993) 189.
24. W. J. BOETTINGER, A. A. WHEELER, B. T. MURRAY, G. B. McFADDEN and R. KOBAYASHI, in "Modeling of Casting, Welding and Advanced Solidification Processes—VI", edited by T. S. Piwonka, V. Voller and L. Katgerman (TMS, Florida, 1993) p. 79.
25. M. HILLERT, *Jernkontorets Ann.* **141** (1957) 757.
26. K. A. TILLER, "Liquid Metals and Solidification" (ASM, Cleveland, OH, 1958).
27. K. A. JACKSON and J. D. HUNT, *Trans. Metall. Soc. AIME* **236** (1966) 1129.
28. J. P. CHILTON and W. C. WINEGARD, *J. Inst. Metals* **89** (1961) 162.
29. J. D. HUNT and J. P. CHILTON, *ibid.* **92** (1963) 21.
30. A. MOORE and R. ELLIOT, in "The Solidification of Metals" (Iron and Steel Institute, London, 1968) p. 167.
31. J. LIU and R. ELLIOT, *Mater. Sci. Eng.* **A173** (1993) 129.
32. A. KARMA, *Phys. Rev. Lett.* **59** (1987) 71.
33. R. XIAO, J. IWAN, D. ALEXANDER and F. ROSENBERGER, *Phys. Rev. A* **45** (1992) 571.
34. S. G. R. BROWN and J. A. SPITTLE, *Scripta Metall. Mater.* **27** (1992) 1599.
35. S. G. R. BROWN, T. WILLIAMS and J. A. SPITTLE, *Acta Metall. Mater.* **42** (1994) 2893.
36. S. G. R. BROWN, G. P. CLARKE and A. J. BROOKS, *Mater. Sci. Technol.* (1994) in press.
37. J. A. SPITTLE and S. G. R. BROWN, *Acta Metall. Mater.* (1994) to be published.
38. M. E. GLICKSMAN, R. J. SCHAEFFER and J. D. AYERS, *Metall. Trans. A* **7A** (1976) 1747.

Received 9 June
and accepted 11 August 1994